Robust Automatic Detection of P Wave and T Wave in Electrocardiogram

Dimitrios Zavantis, Ermioni Mastora, George Manis

Department of Computer Science and Engineering, University of Ioannina, Greece

Abstract

The Electrocardiogram (ECG) is a significant tool to investigate the electrical activity of the heart. Even though P and T waves reveal very useful information, their accurate detection is a difficult and challenging task on account of noise, baseline drift and odd morphologies.

The need for a rapid and effective detection algorithm motivated us to propose two automated methods: the percentile based Automatic Detection (pAD) and the Graphical based Automatic Detection (gAD). Both algorithms use statistical and probabilistic concepts to achieve adequate delineation and detection of the waves. The former uses the percentile as an adaptive threshold to define the location of these waves. The latter uses a "feature wavebank" to train a graphical probabilistic model named as Hidden Conditional Random Field (HCRF). The gAD algorithm takes advantage of the monotonicity and the slope of an ECG to detect and collect waves, which imports to the graphical model and classifies them to P or T waves.

The efficiency of our proposed algorithms has been evaluated on 10 long-term (24-hour) ECG recordings of MIT-BIH Normal Sinus Rhythm Database. The training set we used for gAD was very small, only the 0.2% *of the total number of the available waves. The results show a significant and promising detection accuracy rate.*

1. Introduction

The Electrocardiogram represents a non-invasive method which provides crucial information about the functionality and performance of human heart and the influencing factors. The ECG waveform is well characterized by its cyclic behavior of sequential occurrence of P (atrial depolarization), QRS (ventricular depolarization), and T (ventricular repolarization) waves. Obviously, each wave represents a specific physiological performance of the heart system. As a result, a cumulative analysis of ECG wave components is significant in diagnosis and prognosis of abnormalities (morphological pattern changes) or disorder of heart rate and requires the detection of these waves.

In literature, there is a growing number of researches on automatic analysis of ECG signal and delineation of P and T waves. The detection task is challenging due to amplitude and morphology variability, low signal-to-noise ratio (SNR), low amplitudes, and possible overlapping of the P wave and T wave with the QRS complex. There have been different approaches on detection of P and T waves. Murthy and Prasad [1] have used the discrete cosine transform (DCT) for delineation of P waves, whereas Murthy & Niranjan [2] the discrete Fourier transform (DFT). Thakor and Zhu [3] used their own adaptive filter focusing on P waves. Trahanias and Skordalakis [4] applied a syntactic approach to ECG pattern recognition and parameter measurement for the detection of P, QRS and T waves. Martínez *et al*. used an application of the phasor transform for automatic delineation of single-lead ECG fiducial points. Laguna *et al*. [5] and Chatterjee *et al*. [6] illustrate techniques for automatic detection of wave boundaries based on slope estimation. Madeiro *et al*. [7] proposed a mathematical modeling of P and T wave. There are instances of studies in literature for P and T waves detection, which have used multi-resolution wavelet analysis [8–14], ensemble averaging [15], sparse derivatives [16], nonlinear transform [17] and correlation analysis [18].

However, building a reliable and powerful method for automatic ECG delineation is still far from being solved and remains a topic of main interest.

2. Data and Methods

2.1. Data

The efficiency of our proposed algorithms has been evaluated on 10 long-term (24-hour) ECG recordings of *MIT-BIH Normal Sinus Rhythm Database*. The subjects had no significant arrhythmia with age range from 20 to 50. The database is sampled at 128 Hz and the data is available at uniform intervals of 7.8125 msec [19].

2.2. Preprocessing

Initially, the signals are preprocessed to eliminate the undesirable frequencies (parasitic, noises). To achieve that, a moving average filter was implemented to smooth data by replacing each data point with the average of the N neighboring data points. This process is equivalent to

 ISSN: 2325-887X DOI:10.22489/CinC.2017.089-407

lowpass filtering and is given by the following equation:

$$y_s(i) = \frac{1}{2N+1}(y(i+N)+y(i+N-1)+..+y(i-N)),$$

where $y_s(i)$ is the smoothed value for the i_{th} data point and N is the number of neighboring data points (in our case $N = 5$).

The signal has been divided into segments to reduce baseline drift. The detection of P and T waves, with respect to R peak, would be easier if R peaks were preserved unaffected by the filter. Hence, the location and the value of R were used from the original signal and not from the filtered one.

2.3. Percentile Automatic Detection

The *percentile based Automatic Detection (pAD)* consists of three basic steps. The first step is the location of the waves. The peak of each wave has been detected using as threshold the percentile. The k_{th} percentile of the signal is the value below which k percent of the observations may be found. It has been noticed that the intervals $I_T = [90th\ percentile \pm 0.3\ mV]$ and $I_P = [65th\ percentile \pm 0.2\ mV]$ contain a set of values and among them the corresponding peaks of T and P wave. Figure 1 illustrates the percentile area for the selection.

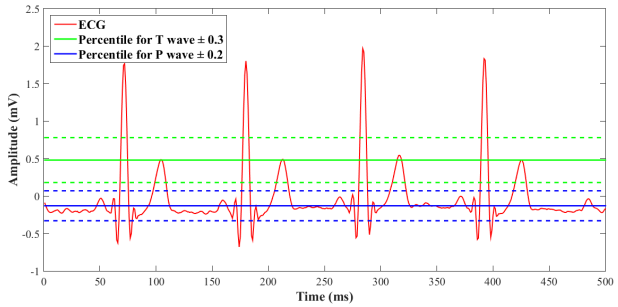

Figure 1. The percentile based Automatic Detection

The second step aims to isolate the peaks by using the set S, which is defined as follows:

$$S = \{x : f(x) \in I_T\ (or\ I_P)\},$$

where $f(x)$ are ECG values and x their locations. The set S has to be divided into subsets S_i, where each contains consecutive elements. Next, the maximum values for subsets, $M = \{maxS_i\}$ were found which are acceptable only if they were not the first or the last element of S_i, to avoid selecting points of the QRS complex. For each R, the peak of M which is 35*7.8125 msec after R or 25*7.8125 msec before R was kept. Finally, the set $M' = \{maxS_i\}$ consists of the location of the peaks.

For each peak we move to the right until the gradient stops to be negative and we consider this point the end of the wave. The start is the point on the left part of the wave having the closest ordinate with the ending point.

This approach has the opportunity to select the waves that are within the area defined by percentile values with excellent results for both P and T waves. However, in most cases an ECG signal has a shifted baseline across the time (change in mV). Hence, the next method has been created to achieve better results defying those shifts among other things that will be discussed below.

2.4. Graphical based Automatic Detection

The morphology of the waves provides a lot of information and can be used to classify the waves to their corresponding group based on their differences. As a result, a training set of feature vectors of P and T waves has been created using an adequate number of waves, collected by the *pAD* method. The feature vector represents four estimated morphological features: area, height, left slope and right slope.

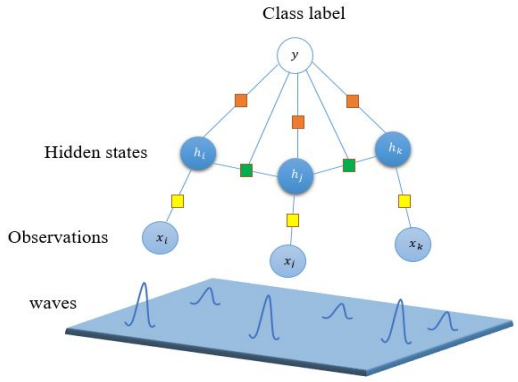

Figure 2. The HCRF graphical model

Given a training set $(x_1, y_1), (x_2, y_2), ..., (x_m, y_m)$, where x_i denotes the feature vector described above and y_i is the class label for every wave (P or T), the *Hidden Conditional Random Field (HCRF)* model [20] has been employed for the classification (Figure 2). The classification task aims to map each observation sequence to its actual label. An HCRF models the conditional probability of a class label given an observation sequence as follows:

$$P(y, h|x, \theta) = \frac{\exp \Psi(y, h, x; \theta)}{\sum_{y' \in \mathcal{Y}} \sum_h \exp \Psi(y', h, x; \theta)}, \quad (1)$$

where $h = \{h_1, h_2, ..., h_m\}$ are the hidden states. Hidden states are not observable during the training phase and are assigned to each observation in order to capture certain underlying structure of each class. Moreover, the *HCRF* algorithm requires the number of hidden states to

be assigned in advance by the user. The potential function $\Psi(y, h, x; \theta)$, which is parametrized by θ, measures the compatibility between a label, a configuration of the hidden states and an observations.

Training and Inference: Given a new test wave x, and parameter values $\theta^\star$ induced from training set, the inferred label for the new wave will be:

$$y^\star = \arg\max P(y|x; \theta^\star). \quad (2)$$

The objective function used in training phase is defined below:

$$\mathcal{L}(\theta) = \log P(y|x; \theta) - \frac{1}{2\sigma^2}\|\theta\|^2, \quad (3)$$

as the difference of conditional log-likelihood term and a penalty term. The penalty term assumes the model parameter follows a normal distribution $P(\theta) \sim N(0, \sigma^2)$ to constrain the $\|\theta\|$. The optimal $\theta^\star$ which maximizes the $\mathcal{L}$ can not be computed analytically; instead we have employed LBFGS, an iterative method to estimate it.

Classification: The waves, which will be used for the test phase have been selected in three stages. The first stage (Figure 3) is the determination of the start-to-peak of the waves. In this stage we include values of ECG with positive first derivative and denote these values as the first half of the wave (onset to peak).

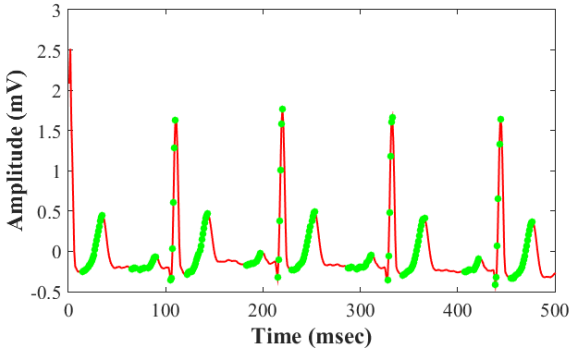

Figure 3. Detection of onset-to-peak of the waves

In the second stage (Figure 4) we eliminate values of QRS complex and noise, which have been selected in the earlier stage. The left fitting slope has been calculated and used as a constrain for the elimination. The range of the slope will be specified. Its minimum value has been defined as the minimum of left fitting slope for both P and T waves for all patients, whereas the maximum threshold value as the maximum left fitting slope.

Finally, to detect the other half wave (Figure 5), an addendum of half of the length of current wave has been implemented to locate the maximum value (the peak). Having fixed the peak, values of ECG with negative first derivative on the right side of the peak have been denoted as the second half of the wave (peak to offset).

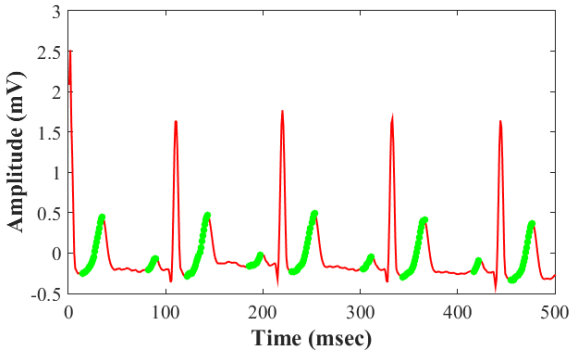

Figure 4. Remove of QRS and noise

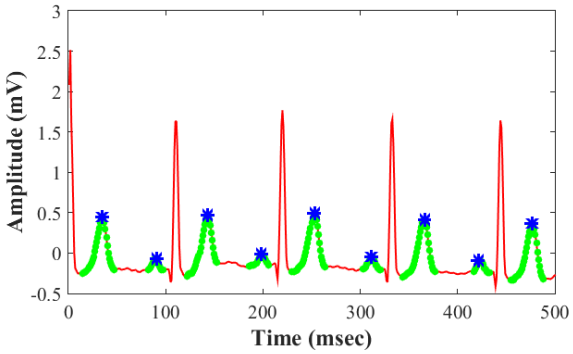

Figure 5. Detection of peak-to-offset of the waves

3. Results

The total number of selected waves for both methods are shown in Table 1. Each line is for a different subject, while the last line shows the average classification accuracy. For the *gAD* algorithm, a cross-validation process has been implemented to find the optimal number of hidden states for HCRF, which is four in our case. As we may notice all P or T wave values from the *pAD* algorithm are less than those from the *gAD* algorithm respectively. The intuition of these percentages (e.g. in 97%) is to declare that among 100K R peaks the 97K waves have been detected correctly. The other 3K may not be even present or can not be detected due to variability and odd morphology. A check for false records is implemented in every subject respectively using as criterion the R peak annotation. As a consequense, the results of this table show only the correct waves from both algorithms.

4. Conclusion

In this paper we present two automatic methods for the detection of P and T waves. The *pAD* is applied to the ECG wave using as threshold the percentile concept. The set of values in that interval include the area where the peaks and

Table 1. Accuracy rate of detected waves

pAD		gAD	
P wave	T wave	P wave	T wave
40.75%	45.73%	77.22%	88.72%
34.47%	31.19%	69.66%	78.35%
55.87%	57.01%	97.10%	95.33%
23.18%	51.22%	63.75%	61.66%
50.60%	60.55%	94.74%	99.00%
20.91%	47.16%	66.25%	65.45%
22.94%	26.53%	67.45%	69.31%
25.58%	36.93%	68.32%	76.33%
24.06%	60.74%	76.29%	77.97%
19.31%	41.69%	77.21%	86.13%
31.76%	45.87%	75.79%	79.82%

consequently the waves may be available. Due to noise, baseline drift or odd morphologies the *gAD* method is proposed in which a small amount of waves has been been selected as the training set. Utilizing the *HCRF* as a classification method, the detection has achieved high accuracy rate and a sufficient number of waves which can be used for further analysis.

References

[1] Murthy I, Prasad GD. Analysis of ECG from pole-zero models. IEEE Transactions on Biomedical Engineering 1992;39(7):741–751.

[2] Murthy I, Niranjan U. Component wave delineation of ECG by filtering in the fourier domain. Medical and Biological Engineering and Computing 1992;30(2):169–176.

[3] Thakor NV, Zhu YS. Applications of adaptive filtering to ECG analysis: noise cancellation and arrhythmia detection. IEEE transactions on Biomedical Engineering 1991; 38(8):785–794.

[4] Trahanias P, Skordalakis E. Syntactic pattern recognition of the ECG. IEEE Transactions on Pattern Analysis and Machine Intelligence 1990;12(7):648–657.

[5] Laguna P, Jané R, Caminal P. Automatic detection of wave boundaries in multilead ECG signals: Validation with the CSE database. Computers and Biomedical Research 1994; 27(1):45–60.

[6] Chatterjee H, Gupta R, Mitra M. Real time P and T wave detection from ECG using FPGA. Procedia Technology 2012;4:840–844.

[7] Madeiro JP, Nicolson WB, Cortez PC, Marques JA, Vázquez-Seisdedos CR, Elangovan N, Ng GA, Schlindwein FS. New approach for T-wave peak detection and t-wave end location in 12-lead paced ECG signals based on a mathematical model. Medical Engineering Physics 2013;35(8):1105–1115.

[8] Li C, Zheng C, Tai C. Detection of ECG characteristic points using wavelet transforms. IEEE Transactions on Biomedical Engineering 1995;42(1):21–28.

[9] Martínez JP, Almeida R, Olmos S, Rocha AP, Laguna P. A wavelet-based ECG delineator: evaluation on standard databases. IEEE Transactions on Biomedical Engineering 2004;51(4):570–581.

[10] Ghaffari A, Homaeinezhad M, Akraminia M, Atarod M, Daevaeiha M. A robust wavelet-based multi-lead electrocardiogram delineation algorithm. Medical Engineering Physics 2009;31(10):1219–1227.

[11] Pal S, Mitra M. Detection of ecg characteristic points using multiresolution wavelet analysis based selective coefficient method. Measurement 2010;43(2):255–261.

[12] Homaeinezhad MR, Ghaffari A, Toosi HN, Tahmasebi M, Daevaeiha M. Optimal delineation of ambulatory holter ECG events via false-alarm bounded segmentation of a wavelet-based principal components analyzed decision statistic. Cardiovascular Engineering 2010;10(3):136–156.

[13] Ghaffari A, Homaeinezhad MR, Daevaeiha MM. High resolution ambulatory holter ECG events detection-delineation via modified multi-lead wavelet-based features analysis: Detection and quantification of heart rate turbulence. Expert Systems with Applications 2011;38(5):5299–5310.

[14] Banerjee S, Mitra M. Application of cross wavelet transform for ECG pattern analysis and classification. IEEE Transactions on Instrumentation and Measurement 2014; 63(2):326–333.

[15] Naseri H, Pourkhajeh H, Homaeinezhad MR. A unified procedure for detecting, quantifying, and validating electrocardiogram T-wave alternans. Medical Biological Engineering Computing 2013;51(9):1031–1042.

[16] Ning X, Selesnick IW. ECG enhancement and qrs detection based on sparse derivatives. Biomedical Signal Processing and Control 2013;8(6):713–723.

[17] Suppappola S, Sun Y. Nonlinear transforms of ECG signals for digital QRS detection: a quantitative analysis. IEEE Transactions on Biomedical Engineering 1994;41(4):397–400.

[18] Homaeinezhad MR, ErfanianMoshiri-Nejad M, Naseri H. A correlation analysis-based detection and delineation of ECG characteristic events using template waveforms extracted by ensemble averaging of clustered heart cycles. Computers in Biology and Medicine 2014;44:66–75.

[19] Goldberger AL, Amaral LA, Glass L, Hausdorff JM, Ivanov PC, Mark RG, Mietus JE, Moody GB, Peng CK, Stanley HE. Physiobank, physiotoolkit, and physionet. Circulation 2000;101(23):e215–e220.

[20] Quattoni A, Wang S, Morency LP, Collins M, Darrell T. Hidden conditional random fields. IEEE Transactions on Pattern Analysis and Machine Intelligence 2007;29(10).

Address for correspondence:

George Manis

Dept. of Computer Science and Engineering, University of Ioannina, P.O. Box 1186, 45110, Ioannina, Greece

manis@cs.uoi.gr